2020 IEEE/RSJ International Conference on Intelligent Robots and Systems (IROS)
October 25-29, 2020, Las Vegas, NV, USA (Virtual)

Laminar Jamming Flexure Joints for the Development of Variable Stiffness Robot Grippers and Hands

Lucas Gerez, Geng Gao, and Minas Liarokapis

***Abstract*— Although soft robots are a good alternative to rigid, traditional robots due to their intrinsic compliance and environmental adaptability, there are several drawbacks that limit their impact, such as low force exertion capability and low resistance to deformation. For this reason, soft structures of variable stiffness have become a popular solution in the field to combine the benefits of both soft and rigid designs. In this paper, we develop laminar jamming flexure joints that facilitate the development of adaptive robot grippers with variable stiffness. Initially, we propose a mathematical model of the laminar jamming structures. Then, the model is experimentally validated through bending tests using different materials, pressures, and number of layers. Finally, the soft, laminar jamming structured are employed to develop variable stiffness flexure joints for two different adaptive robot grippers. Bending profile analysis and grasping tests have demonstrated the benefits of the proposed jamming structures and the capabilities of the designed grippers.**

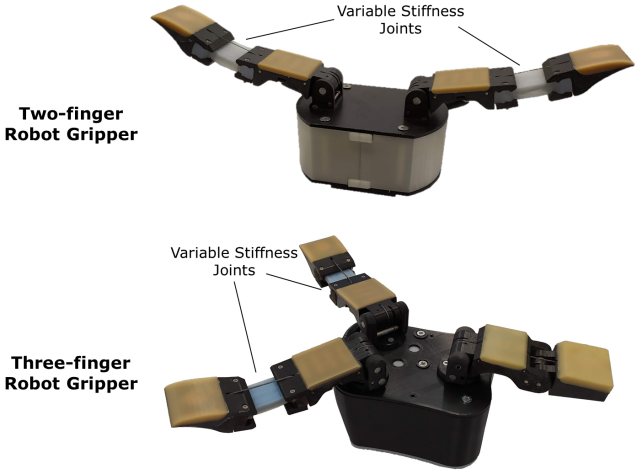

Fig. 1. Two adaptive robot grippers have been developed using laminar jamming flexure joints. The jamming structure allows for control of the stiffness of each joint. The top subfigure presents the two-fingered gripper, while the bottom subfigure presents the three-fingered gripper.

I. Introduction

Over the last decade, the soft robotics field has received an increased interest from the research community. Robots have evolved from rigid mechanisms to soft, flexible, and customized systems [1]. The success and popularity of soft robots are due to the intrinsic mechanical properties (e.g., compliance) of soft materials that provide high environmental adaptability, conforming to complex shapes, and withstanding significant crushing loads. For this reason, the materials applied in soft robots play an important role in the behaviour and the capabilities of this class of robots. Although soft materials can assist robots in adapting to the object's geometry and grasp fragile items, they suffer from several drawbacks, such as low control accuracy, low force exertion capability, and low resistance to deformation [2].

In order to overcome these disadvantages, researchers have developed methods to selectively control the stiffness of soft structures. Depending on the selected material and working principle of the variable stiffness module, stiffness can be controlled by varying the temperature, electrical current, pressure, and magnetic field of the device. Such structures can be used in devices applied in the medical industry, structural engineering, automotive, and aerospace industries [3]. In [4], the authors propose a shape memory alloy-based soft gripper, which can control the stiffness of the joints, increasing the grasping force ten times. The limitation of shape memory alloy (SMA) and shape memory polymer (SMP) structures is their low response speed due to the high amount of time required to change the material temperature and, therefore, its stiffness [5], [6]. In [7], the authors present a robot gripper that utilizes the effects of a magnetorheological (MR) fluid (viscosity changes according to the magnetic field applied) to conform the fingerpad of the gripper to the object's shape. The limitation of MR fluids is that they require heavy electromagnets to generate sufficient magnetic flux density for the solidification of the MR fluid [8]. Additionally, the use of a magnetic field can limit interactions with magnetically sensitive materials / objects, potentially damaging them in the process. In [9], the authors propose voltage-actuated dielectric elastomer beams that can be used to grasp several objects. However, the deformation and change in stiffness achieved by the dielectric elastomer actuators (DEA) are not enough to withstand more than a few grams of weight [10], [11].

Another method for tuning stiffness of soft structures is by applying a pressure gradient into a closed system (e.g., pouch) and relying on the contact between solid parts to alter the stiffness of the soft structure. In [12], the authors propose a joint assistance device based on the jamming of granular parts. Rubber granules are filled into a silicone sleeve, and the pressure change inside the sections varies the stiffness of the device. In [13], the authors combine a granular jamming structure with pneumatic soft actuators to increase the efficiency of a soft gripper and the resisting load by more than ten times when a vacuum is applied.

Lucas Gerez, Geng Gao, and Minas Liarokapis are with the New Dexterity research group, Department of Mechanical Engineering, The University of Auckland, New Zealand. E-mails: lger871@aucklanduni.ac.nz, ggao102@aucklanduni.ac.nz, minas.liarokapis@auckland.ac.nz

Granular jamming structures, however, do not withstand high tensile and bending loads, having limited applications. On the other hand, laminar jamming structures (stack of flexible layers to which an external pressure gradient is applied) can offer more resistance to tensile stress and tensile bending stress due to the direction of applied frictional forces being parallel to these stresses. This can be seen when comparing jamming structures for the design of manipulators, as a laminar jamming manipulator [14] is capable of resisting more than 2 times the load of a granular jamming manipulator [15]. In [16], the authors describe several applications of tunable stiffness using laminar jamming structures. These applications can range from the development of variable stiffness furniture to the creation of variable softness sports shoes. In [17], the authors incorporate laminar jamming into soft, tendon-driven fingers to improve their force exertion capabilities during grasping. In [18], the authors propose a laminar jamming structure to tune dynamic responses of robotic systems by increasing stiffness by more than 20 times when a vacuum is applied to the envelope.

In this paper, we propose laminar jamming flexure joints that can be used to develop adaptive robot grippers with variable stiffness. Initially, we discuss the designs and the mathematical modelling. Then, the model is experimentally validated through bending tests using different materials, pressures, and number of layers. The efficiency of the proposed jamming structures is experimentally validated by controlling the stiffness of the flexure joints of two adaptive robot grippers (Fig. 1). Bending profile analysis and grasping tests were performed to evaluate the effect of the jamming structures on the capabilities of the grippers.

The rest of the paper is organized as follows: Section II presents the designs, Section III details the experimental setup used and presents the results, while Section IV concludes the paper and discusses future directions.

II. Soft Laminar Jamming Structure

In this section, we present the designs and the modelling of the laminar jamming structures.

A. Design

The soft, laminar jamming structure was designed to achieve multiple stiffnesses by applying a pressure gradient into the system. The structure is composed of a soft pouch with several thin layers inside it (see Fig. 2). When the vacuum is applied inside the pouch, the high friction between layers increase the yield point of the entire structure. The pouches tested in this study are made out of silicone rubber (Smooth-On Dragon Skin 30), and their walls are 1 mm thick. The bending tests used pouches 142 mm long, 11 mm high, and 26 mm wide.

There are several parameters that can change the performance of laminar jamming structures [19]. In this study, we verify the effect of the layers' material, the number of layers, and the system pressure in the behaviour of the jamming structure. Four different layer materials were analyzed (see Fig. 3): white paper (0.1 mm thick), sandpaper P800 (0.20 mm thick), sandpaper P360 (0.22 mm thick), and sandpaper P150 (0.32 mm thick). These materials were chosen because they provide high friction between the layers, which results in stiffer jamming structures. Also, the use of off-the-shelf materials is important for the replication of this study by others and for further analysis. Three different total thicknesses were also analyzed: 4 mm, 6 mm, and 8 mm. The described parameters were tested in three vacuum pressures: 30 kPa, 50 kPa, and 70 kPa.

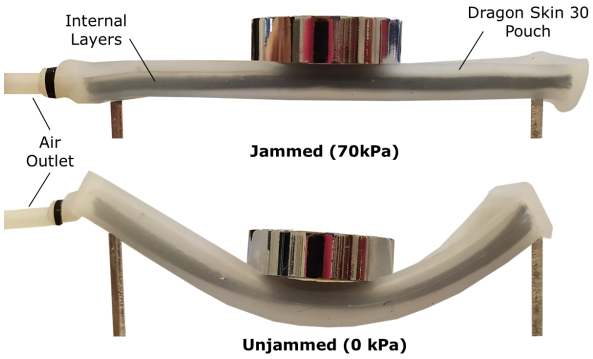

Fig. 2. The soft laminar jamming structure can achieve multiple stiffnesses by applying a pressure gradient into the system. The structure is composed of a soft pouch made out of silicone rubber (Smooth-On Dragon Skin 30), an air outlet, and several thin layers. When the vacuum is applied inside the pouch, the high friction between layers increase the yield point of the entire structure.

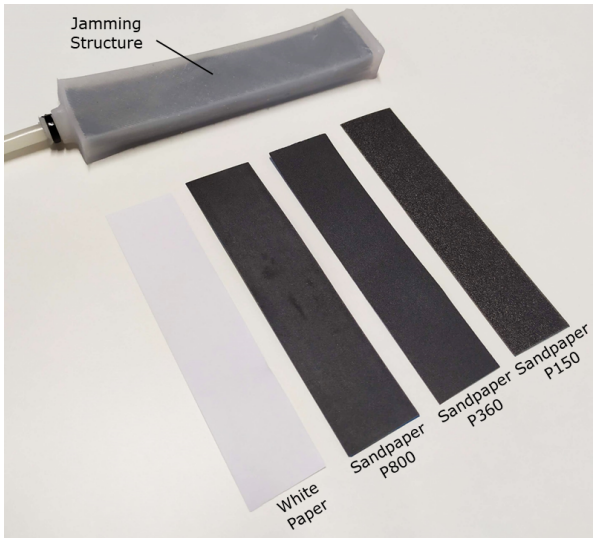

Fig. 3. The soft laminar jamming structure was tested with four different types of layers: white paper (80 gsm), sandpaper P150 grit (coarse), sandpaper P360 grit (medium), and sandpaper P800 grit (fine). Also, three different layer thicknesses were analyzed: 4 mm, 6 mm, and 8 mm. The described parameters were tested in three vacuum pressures: 30 kPa, 50 kPa, and 70 kPa.

B. Analytical Modelling

The correct estimation of the limits of the jamming structure in terms of stiffness capabilities is highly important in order to verify the best jamming structure that fits the desired application. For this reason, an analytical model was developed to estimate the performance of the jamming

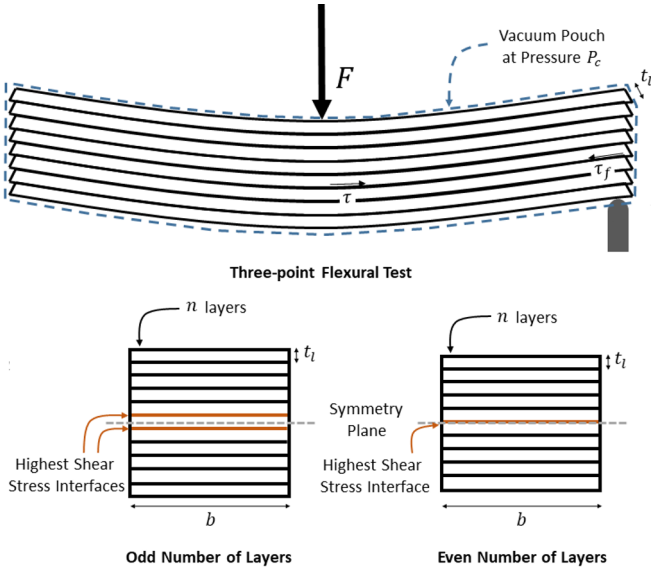

Fig. 4. The proposed model is based on the behaviour of composite beams. The maximum load that can be applied to the jamming structure until its plastic deformation starts, is achieved right before the layers slide between each other. Thus, the shear stress calculated should be less than the maximum frictional stress to guarantee that the layers will not slip between each other. The maximum shear stress between layers is obtained close to the symmetry plane / neutral axis (between the center layer and the adjacent layer). When the number of layers is even, the maximum shear stress is applied to the interface of the two middle layers where the symmetry plane is located. When the number of layers is odd, the maximum shear stress is applied to the closest interface to the symmetry plane.

structure according to the available vacuum pressure of the system. The proposed model can be used to improve the design of the actuator by testing multiple materials and geometries (for future design iterations), without manufacturing physical prototypes. Also, it can be used for controlling the stiffness of a robotic system in a closed-loop manner. Finite-element simulations can become computationally expensive with jamming structures that have numerous layers [20].

One of the most popular tests to analyze the properties and behaviour of materials is the three-point flexural test. Thus, we propose an analytic model considering the conditions of this test. We propose a model based on the behaviour of composite beams. A composite beam is composed of two or more elemental structural forms, or different materials joined together. In this model, we assume that the material is uniform and that the jamming structure is symmetric. Previous experiments with jamming structures [20], have demonstrated that the maximum vertical elastic deformation of this kind of structure is less than 10% of the length of the layers. Thus, the Euler–Bernoulli beam theory [21] can be adopted to model this structure. The problem can be divided into two different parts: before and after the layers slide between each other. The maximum load that can be applied to the jamming structure until its plastic deformation starts, is achieved right before the layers slide between each other.

Considering a force F being applied at the center of the structure during a three-point flexural test (Fig. 4), the shear stress, τ, can be calculated by

$$\tau = \frac{VQ}{I_{eq}b}, \tag{1}$$

Where V is the shear force at the point, Q is the first moment of area, I is the equivalent moment of inertia of the entire cross-section area, and b is the width of the layer. The shear stress calculated should be less than the maximum frictional stress to guarantee that the layers will not slip between each other. According to Eq. 1, the maximum shear stress in between layers is obtained close to the symmetry plane / neutral axis (between the center layer and the adjacent layer). The frictional stress, τ_f, can be calculated by dividing the friction force by the area of the interface, A_l, using the Eq. 2. More precisely, μ_s is defined as the static friction coefficient between both layers. The ratio between the normal force, N_f, and the area of the interface can be written as the vacuum pressure, P_c, in the jamming structure. The weight of layers was neglected in the normal force calculation.

$$\tau_f = \frac{\mu_s N_f}{A_l} = \mu_s P_c \tag{2}$$

Thus, the maximum shear force, V_{yield}, before the layers slip in the interface can be calculated using the following equation (Eq. 3). The shear force can also be written in terms of the yield force, F_{yield}, as follows

$$V_{yield} = \frac{F_{yield}}{2} = \frac{\mu_s P_c I b}{Q} \tag{3}$$

The first moment of area, Q, when the structure is under vacuum, can be calculated (for n number of layers) in the interface with the highest shear stress (Fig. 4). If the number of layers is odd, the moment of area is defined as

$$Q_{odd} = \frac{(n^2-1)bt_l^2}{8}, \tag{4}$$

Where t_l is the thickness of each layer. If the number of layers is even, the moment of area is defined as

$$Q_{even} = \frac{n^2 bt_l^2}{8}. \tag{5}$$

The equivalent moment of inertia of the structure under vacuum can be calculated using Eq. 6, as follows

$$I = \frac{n^3 bt_l^3}{12} \tag{6}$$

Combining Eq. 4 or Eq. 5 and Eq. 6 in Eq. 3, the yield force for a three-point flexural test can be written as

$$F_{even} = \frac{4nbt_l \mu_s P_c}{3}, \tag{7}$$

For an even number of layers, and

$$F_{odd} = \frac{4n^3 bt_l \mu_s P_c}{3(n^2-1)}, \tag{8}$$

For an odd number of layers. Analyzing Eq. 7 and Eq. 8, it can be noticed that the force required to slide the layers of the jamming structure (yield force) is directly proportional

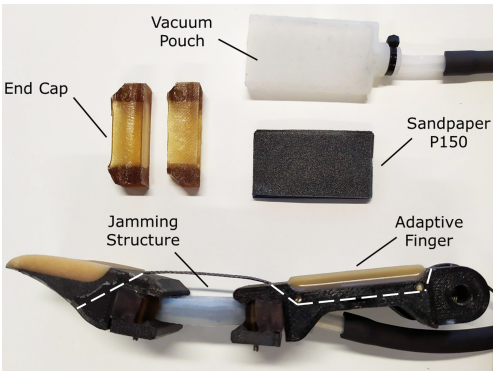

Fig. 5. This adaptive, variable stiffness, robotic finger consists of a laminar jamming flexure joint (based on a vacuum pouch made from SmoothOn Dragon skin 30) with ten P150 grit sandpaper layers, two urethane end caps (SmoothOn PMC-780), and two phalanges. The white dashed line shows the tendon routing channels of the finger.

to the friction coefficient between the layers and the vacuum pressure applied to the system. Moreover, the yield force increases with the number of layers, and when very thin layers are used, the yield force equations for odd and even number of layers provide similar results.

C. Adaptive Grippers with Variable Stiffness

Adaptive robot grippers are a popular solution for performing object grasping and dexterous manipulation due to their ability to execute stable grasps even under object pose uncertainties, their low complexity, robustness, and affordability. Adaptive robot grippers are able to replace complex, heavy, and expensive robot devices that require sophisticated sensing and complicated control laws [22], [23]. Their efficiency is due to the structural compliance and the underactuation that allow them to adjust their grasping postures according to the object geometry, maximizing the area of contact with the object [24], [25]. Despite the outstanding performance, adaptive grippers have also certain drawbacks and limitations. An underactuated design is characterized by a significant post-contact reconfiguration of the hand object system that imposes a parasitic object motion. This reconfiguration occurs until the system reaches an equilibrium configuration [26], and it may compromise the pinch grasping capabilities of the system. For this reason, adaptive hands are typically used for full / power grasps, and they are not very efficient in the execution of pinch grasps. Although underactuated fingers can be optimized for joint stiffness, link length ratios, and tendon routing for specific configurations, this cannot prevent reconfiguration in all finger configurations and contact force points. By implementing variable stiffness flexure joints, a higher number of finger configurations / poses can be achieved, enabling more manipulation profiles to be executed by compliant and underactuated robot hands.

In a previous work [27], we have demonstrated that during a pinch grasp, a significant amount of the applied load is wasted on reconfiguration. This reduces the available fingertip force that could be applied to the object, compromising the overall grasp efficiency. By adjusting the stiffness of the joints, it is possible to increase the force applied by the gripper in pinch grasps. Thus, in this paper, we have developed two adaptive robot grippers (a two-fingered and a three-fingered design) that employ the proposed laminar jamming flexure joints to increase their grasping capabilities.

1) A Two Fingered Adaptive Robot Gripper: The first adaptive robot gripper consists of two robot fingers with two phalanges each and a robot base. Artificial tendons connect the fingertip of the robotic fingers to motors (Dynamixel XM430-W350-R) located at the gripper base (see Fig. 5). The finger structure is inspired by the Model T42 gripper [28]. The joints of the fingers consist of a set of pin joints at the metacarpophalangeal (MCP) joints, and modular, laminar jamming flexure structures that act as the distal interphalangeal (DIP) joints. This allows for the exertion of high pinch grasp forces, while ensuring that the stiffness of the joints does not reduce the efficiency of the power grasp. The jamming flexure joints consist of ten P150 grit sandpaper layers encased in a silicone vacuum pouch (SmoothOn Dragon Skin 30). Urethane end caps (SmoothOn PMC-780) fitted to the ends of the pouch are clamped to the edges of the finger phalanges to distribute load through the laminar layer while providing a tight seal. The described finger and its construction can be seen in Fig. 5. A single vacuum pressure actuator is used to jam the layers of both fingers, enabling variable stiffness at the DIP joint. This provides increased controllability over finger poses while maintaining the compliant attributes of conventional flexure joints.

2) A Three Fingered Adaptive Robot Gripper: The second adaptive robot gripper consists of three robot fingers with two phalanges each and a robot base. The design employs the same tendon-driven actuation scheme and similar motors (Dynamixel MX28-AR) located at the gripper base. The finger structure is inspired by the Model O gripper [28]. The joints of the fingers consist once again of a set of pin joints at the MCP joints and modular, laminar jamming flexure joints for the DIP joints. The laminar jamming flexure joints are similar to the two-fingered gripper jamming joints and follow the same working principle. Both the two-fingered gripper and the three-fingered gripper are presented in Fig. 1.

III. Experiments and Results

The experiments that were conducted to assess the performance of the jamming structure were divided into four different parts. The first part of the experiments focused on evaluating the laminar jamming structure in different scenarios and validating the proposed mathematical model of the mechanism. The second experiment focused on evaluating the effect of the proposed jamming structure in the bending profile of the robotic fingers. The third part of the experiments assessed the grasping forces of a gripper in different scenarios employing the proposed jamming structure. Finally, the fourth part of the experiments focused on the evaluation of the grasping capabilities of the grippers.

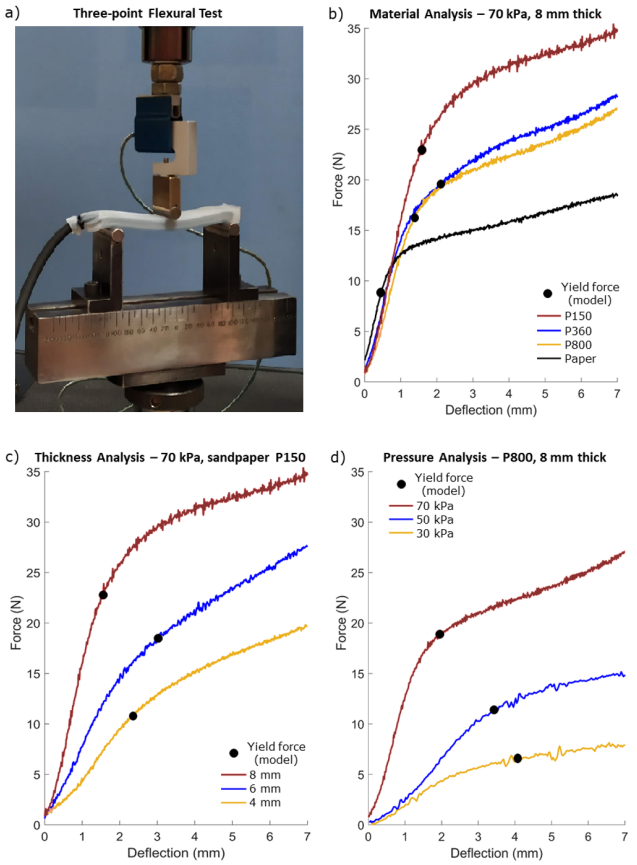

Fig. 6. Laminar jamming structural force vs deflection tests. Subfigure a), shows the three-point flexural test executed using a materials testing machine (Instron 5567) for four different materials, three different thicknesses, and three different pressures. Subfigure b), shows the relationship between the structural deflection and the force for the white paper, the sandpaper P150, the sandpaper P360, and the sandpaper P800, for a combined layer thickness of 8 mm under a pressure of 70 kPa. The force resistance increases with the friction coefficient between the layers. Subfigure c), shows the relationship between the resistance force and the combined thickness of the layers for the sandpaper P150 material at a pressure of 70 kPa. Subfigure d), shows the effect of different pressures on the jamming structure for sandpaper P800 and a combined thickness of the layers of 8 mm.

A. Bending Tests

The first part of the experiments tested different laminar jamming structures by varying the total thickness of the layers (4 mm, 6 mm, and 8 mm) and the layers materials (white paper, sandpaper P150, sandpaper P360, and sandpaper P800). All the different tested conditions were compared to the proposed model (Section II-B). Also, it was tested under vacuum pressures of 30 kPa, 50 kPa, and 70 kPa. The laminar jamming structure was characterized using a materials testing machine (Instron 5567, Instron Limited, UK) through a three-point flexural test (Fig. 6-a). The experiments followed the guidelines of the standard ASTM D790-17 Procedure B (Standard Test Methods for Flexural Properties of Unreinforced and Reinforced Plastics and Electrical Insulating Materials). A total of five trials of each scenario were tested. A 12V vacuum pump was used to apply the pressure gradient and a pressure gauge was used to control the system pressure during the experiments.

TABLE I

STATIC FRICTION COEFFICIENTS (μ_s) AND STANDARD DEVIATION (SD) FOR THE MATERIALS TESTED: WHITE PAPER, SANDPAPER P150 (COARSE), SANDPAPER P360 (MEDIUM), AND SANDPAPER P800 (FINE).

Layer Material	μ_s	SD
White paper	0.38	0.02
Sandpaper P800	0.93	0.03
Sandpaper P360	1.15	0.04
Sandpaper P150	1.32	0.04

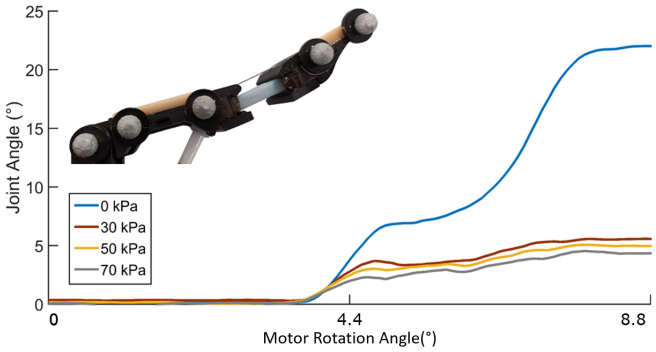

Fig. 7. The joint tracking experiment focused on evaluating the effect of the proposed jamming structure in the bending profile of the robotic fingers. Vacuum pressures of 30 kPa, 50 kPa, and 70 kPa at the DIP joint were used. The results demonstrate that the jamming structure can control the joint angle by applying different vacuum pressure at the jamming structure.

In order to compare the bending test results and the analytical model, it was required to estimate the friction coefficient between the layers of the jamming structure. Thus, friction coefficient tests were performed for all tested materials following the guidelines of the standard ASTM G115 (Standard Guide for Measuring and Reporting Friction Coefficients). The friction coefficients obtained are reported in Table I. Fig. 6 illustrates the results obtained during the experiments. It can be noticed that the yield force of the jamming structure increases as the friction coefficient between the layers (Fig. 6-b), the number of layers (Fig. 6-c), and the vacuum pressure increase (Fig. 6-d). The sandpaper P150 jamming structure offered the best result in terms of force resistance. Also, it was noticed that the motion between the layers gradually changes the ratio between the applied force and the deflection of the structure. The yield force calculated by the proposed analytical model estimated the layer slipping region. The model can be used to improve the design of the jamming structure, testing multiple materials and geometries (for future design iterations) without manufacturing physical prototypes. The model can be also used for controlling the maximum force of jamming structure in closed-loop systems by varying the pouch pressure.

B. Joint Tracking Experiment

The second experiment focused on evaluating the effect of the proposed jamming structure in the bending profile of the robotic fingers. More precisely, it involved the analysis of the bending profile of the finger of the gripper under vacuum pressures of 30 kPa, 50 kPa, and 70 kPa at the

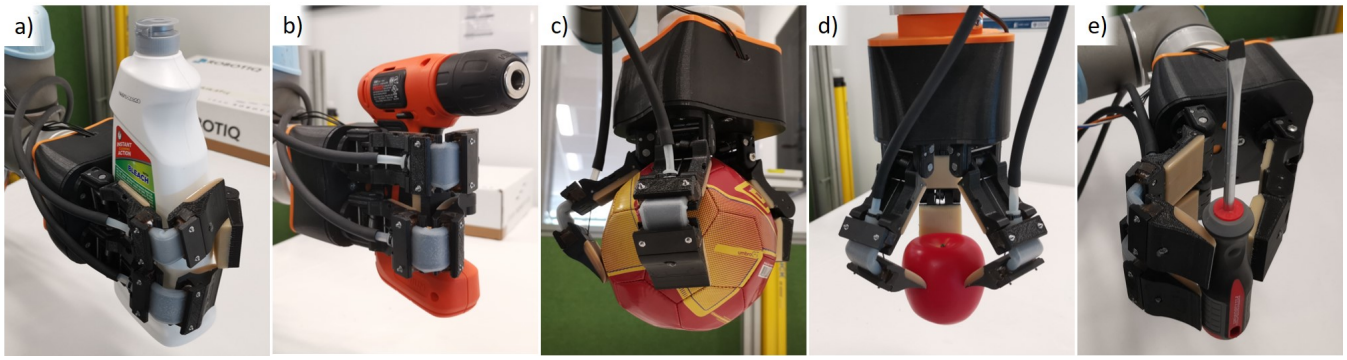

Fig. 8. The three-fingered adaptive robotic gripper with the laminar jamming based flexure joints while executing grasping experiments with everyday objects. The ability of the jamming flexure joints to vary their stiffnesses allows the gripper to bend and grasp with different finger poses.

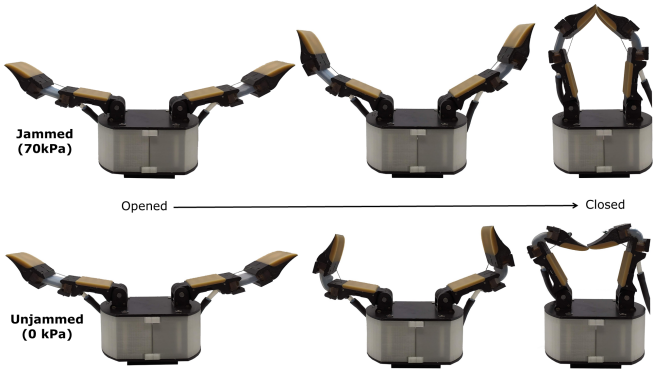

Fig. 9. Gripper motion when the jamming structure is activated (70 kPa) and when it is unjammed (0 kPa). The change in joint behaviour allows the gripper to grasp a wider range of objects by planning the gripper motion prior to the grasp.

DIP joint. The experiment was conducted using an optical motion capture system with eight cameras (Vicon Motion System Ltd., UK) to capture the range of motion of one finger in all four scenarios. Five reflective markers were attached at the side of the robot finger to track its bending profile. In all the trials, the motor was set to the same displacement to guarantee that the tendon had the same displacement independently of the pressure in the jamming structure. The experiment was repeated ten times for each vacuum pressure. Fig. 7 shows DIP joint values for each scenario tested. The results demonstrate that the bending profile of the finger is affected by the vacuum pressure in the jamming structure. When the jamming structure is not under vacuum the DIP joint bends more than 20° before closing completely. Once a vacuum is applied (70 kPa), the joint angle flexion is reduced to less than 5°. However, the finger DIP joint angle trajectory is similar across differing applied vacuum pressures (30 kPa, 50 kPa, and 70 kPa) as the laminar jamming structure will remain at the same stiffness, but the yield force will be altered under negative pressure. Hence, the maximum applied pinch contact force that can be applied can be controlled by altering the yield force of the laminar jamming joint. Fig. 9 shows the gripper motion when the jamming structure is activated and when it is unjammed (0 kPa). This behaviour allows the proposed robotic grippers to approach the objects to be grasped with different fingertip orientations and to execute different grasping strategies. It also allows the robotic gripper to successfully grasp a wider range of everyday objects by planning the gripper motion prior to execution of the grasp.

TABLE II

PINCH FORCE RESULTS FOR THE LAMINAR JAMMING FLEXURE JOINT WITH SANDPAPER P150 GRIT LAYERS UNDER DIFFERENT PRESSURE VALUES.

Vacuum Pressure	Max Pinch Force (N)
0 kPa	0.85
30 kPa	1.19
50 kPa	1.53
70 kPa	2.39

C. Grasping Force Experiment

The third part of the experiments evaluated the effect of the jamming structure on the pinch forces exerted by a robotic gripper. The experiment involved pinch grasping of a dynamometer under different pressures in the jamming structure. A Biopac MP36 data acquisition unit (Biopac Systems, Inc., California, USA) was used with the SS25LA dynamometer to measure the forces exerted in each scenario. The motors were set to the same displacement at all times. Fig. 9 shows the behaviour of the gripper while pinch grasping the dynamometer at the pressure of 0 kPa, 30 kPa, 50 kPa, and 70 kPa in the jamming structure. A total of three trials were executed for each scenario. The results shown in Table II, demonstrate that the gripper can exert higher pinch forces when the jamming structure is subjected to higher pressures (an increase of almost three times in pinch forces was observed compared to a pressure of 0 kPa). When under vacuum, the jamming structure reduces significantly the amount of motor load wasted on finger reconfiguration, resulting in higher pinch forces. Higher pinch forces mean that heavier objects can be grasped and, therefore, more tasks can be executed with the proposed gripper.

D. Grasping of Everyday Objects

Finally, the fourth part of the conducted experiments focused on grasping everyday objects with the proposed grippers. Instances of the experiments conducted with the three-fingered gripper grasping a bleach bottle, a drill, a football, a plastic apple, and a screwdriver can be found in Fig. 8. More experiments involving both grippers can be found in the accompanying video.

E. Video Demonstration

A video containing the device description and the experiments can be found at the following URL:

http://newdexterity.org/jamming

IV. Conclusions and Future Directions

In this paper, we proposed laminar jamming flexure joints that can be used to develop adaptive robot grippers with variable stiffness. The efficiency of the proposed jamming mechanism was experimentally validated through three different types of experiments. The soft laminar jamming structure was also tested in a real application by incorporating it into two different robot gripper designs, conducting grasping force experiments and grasping experiments with everyday objects. The experimental results demonstrate that the jamming structure can be efficiently used to tune the stiffness of flexure joints and that it can increase the capabilities of adaptive grippers: i) improving the exerted pinch grasp forces and ii) controlling the bending profile, increasing the number of possible grasping strategies for various objects. Although laminar jamming joints provide increased dexterity when incorporated into adaptive grippers, the variable stiffness joints have low repeatability and durability when they are fabricated with materials like paper and sandpaper. Such materials exhibit significant ware (when they are bent) that results in reduced surface friction between layers or plastic deformation. Regarding future directions, we plan to integrate the laminar jamming structure to a five-fingered adaptive robotic hand with an embedded vacuum pump to tune the stiffness of the joints in a closed-loop manner.

References

[1] S. Kim, C. Laschi, and B. Trimmer, "Soft robotics: a bioinspired evolution in robotics," *Trends in biotechnology*, vol. 31, no. 5, pp. 287–294, 2013.

[2] P. Polygerinos, N. Correll, S. A. Morin, B. Mosadegh, C. D. Onal, K. Petersen, M. Cianchetti, M. T. Tolley, and R. F. Shepherd, "Soft robotics: Review of fluid-driven intrinsically soft devices; manufacturing, sensing, control, and applications in human-robot interaction," *Advanced Engineering Materials*, vol. 19, no. 12, p. 1700016, 2017.

[3] L. Wang, Y. Yang, Y. Chen, C. Majidi, F. Iida, E. Askounis, and Q. Pei, "Controllable and reversible tuning of material rigidity for robot applications," *Materials Today*, vol. 21, no. 5, pp. 563–576, 2018.

[4] W. Wang and S.-H. Ahn, "Shape memory alloy-based soft gripper with variable stiffness for compliant and effective grasping," *Soft robotics*, vol. 4, no. 4, pp. 379–389, 2017.

[5] L. Wang, U. Culha, and F. Iida, "A dragline-forming mobile robot inspired by spiders," *Bioinspiration & biomimetics*, vol. 9, no. 1, p. 016006, 2014.

[6] Y. Yang, Y. Chen, Y. Li, M. Z. Chen, and Y. Wei, "Bioinspired robotic fingers based on pneumatic actuator and 3d printing of smart material," *Soft robotics*, vol. 4, no. 2, pp. 147–162, 2017.

[7] A. Pettersson, S. Davis, J. Gray, T. Dodd, and T. Ohlsson, "Design of a magnetorheological robot gripper for handling of delicate food products with varying shapes," *Journal of Food Engineering*, vol. 98, no. 3, pp. 332–338, 2010.

[8] T. Nishida, Y. Okatani, and K. Tadakuma, "Development of universal robot gripper using mr α fluid," *International Journal of Humanoid Robotics*, vol. 13, no. 04, p. 1650017, 2016.

[9] S. Shian, K. Bertoldi, and D. R. Clarke, "Dielectric elastomer based "grippers" for soft robotics," *Advanced Materials*, vol. 27, no. 43, pp. 6814–6819, 2015.

[10] G.-K. Lau, K.-R. Heng, A. S. Ahmed, and M. Shrestha, "Dielectric elastomer fingers for versatile grasping and nimble pinching," *Applied Physics Letters*, vol. 110, no. 18, p. 182906, 2017.

[11] J. Shintake, B. Schubert, S. Rosset, H. Shea, and D. Floreano, "Variable stiffness actuator for soft robotics using dielectric elastomer and low-melting-point alloy," in *2015 IEEE/RSJ International Conference on Intelligent Robots and Systems (IROS)*. IEEE, 2015, pp. 1097–1102.

[12] S. Hauser, M. Robertson, A. Ijspeert, and J. Paik, "Jammjoint: A variable stiffness device based on granular jamming for wearable joint support," *IEEE Robotics and Automation Letters*, vol. 2, no. 2, pp. 849–855, 2017.

[13] Y. Wei, Y. Chen, T. Ren, Q. Chen, C. Yan, Y. Yang, and Y. Li, "A novel, variable stiffness robotic gripper based on integrated soft actuating and particle jamming," *Soft Robotics*, vol. 3, no. 3, pp. 134–143, 2016.

[14] Y. Kim, S. Cheng, S. Kim, and K. Iagnemma, "Design of a tubular snake-like manipulator with stiffening capability by layer jamming," in *2012 IEEE/RSJ International Conference on Intelligent Robots and Systems*, 2012, pp. 4251–4256.

[15] N. G. Cheng, M. B. Lobovsky, S. J. Keating, A. M. Setapen, K. I. Gero, A. E. Hosoi, and K. D. Iagnemma, "Design and analysis of a robust, low-cost, highly articulated manipulator enabled by jamming of granular media," in *2012 IEEE International Conference on Robotics and Automation*, 2012, pp. 4328–4333.

[16] J. Ou, L. Yao, D. Tauber, J. Steimle, R. Niiyama, and H. Ishii, "jamsheets: thin interfaces with tunable stiffness enabled by layer jamming," in *Proceedings of the 8th International Conference on Tangible, Embedded and Embodied Interaction*, 2014, pp. 65–72.

[17] Y. Gao, X. Huang, I. S. Mann, and H.-J. Su, "A novel variable stiffness compliant robotic gripper based on layer jamming," *ASME Journal of Mechanisms and Robotics*, vol. 12, no. 5, 2020.

[18] Y. S. Narang, A. Degirmenci, J. J. Vlassak, and R. D. Howe, "Transforming the dynamic response of robotic structures and systems through laminar jamming," *IEEE Robotics and Automation Letters*, vol. 3, no. 2, pp. 688–695, 2017.

[19] V. Wall, R. Deimel, and O. Brock, "Selective stiffening of soft actuators based on jamming," in *2015 IEEE International Conference on Robotics and Automation (ICRA)*. IEEE, 2015, pp. 252–257.

[20] Y. S. Narang, J. J. Vlassak, and R. D. Howe, "Mechanically versatile soft machines through laminar jamming," *Advanced Functional Materials*, vol. 28, no. 17, p. 1707136, 2018.

[21] O. Bauchau and J. Craig, "Euler-bernoulli beam theory," in *Structural analysis*. Springer, 2009, pp. 173–221.

[22] L. Birglen, T. Laliberté, and C. M. Gosselin, *Underactuated robotic hands*. Springer, 2007, vol. 40.

[23] D. M. Aukes, B. Heyneman, J. Ulmen, H. Stuart, M. R. Cutkosky, S. Kim, P. Garcia, and A. Edsinger, "Design and testing of a selectively compliant underactuated hand," *The International Journal of Robotics Research*, vol. 33, no. 5, pp. 721–735, 2014.

[24] A. M. Dollar and R. D. Howe, "A robust compliant grasper via shape deposition manufacturing," *IEEE/ASME transactions on mechatronics*, vol. 11, no. 2, pp. 154–161, 2006.

[25] T. Laliberté, L. Birglen, and C. Gosselin, "Underactuation in robotic grasping hands," *Machine Intelligence & Robotic Control*, vol. 4, no. 3, pp. 1–11, 2002.

[26] M. V. Liarokapis and A. M. Dollar, "Post-contact, in-hand object motion compensation with adaptive hands," *IEEE Transactions on Automation Science and Engineering*, 2016.

[27] L. Gerez, G. Gao, and M. Liarokapis, "Employing magnets to improve the force exertion capabilities of adaptive robot hands in precision grasps," in *2019 IEEE/RSJ International Conference on Intelligent Robots and Systems (IROS)*, Nov 2019, pp. 7630–7635.

[28] R. Ma and A. Dollar, "Yale openhand project: Optimizing open-source hand designs for ease of fabrication and adoption," *IEEE Robotics & Automation Magazine*, vol. 24, no. 1, pp. 32–40, 2017.